The prospects of quantum photometry

D. N. Klyshko and A. N. Penin

M. V. Lomonosov State University, Moscow

Usp. Fiz. Nauk **152**, 653–665 (August 1987)

A review is presented of two original methods of calibrating sources and detectors of optical radiation. Their main feature is that they are absolute, i.e., no calibrated devices are employed. Readings are taken in dimensionless units, i.e., number of pulses per photon, when detectors are calibrated, and number of photons per field mode, when sources are calibrated. A new name is proposed for the latter quantity, namely, the *planck*, since it is a natural quantum unit of the basic photometric variable, i.e., spectral radiance of radiation. Both methods are based on a nonlinear-optics effect, namely, parametric scattering of light, observed in birefringent piezoelectric crystals such as lithium niobate. The necessary data on this effect are presented together with the theoretical bases of the methods and the results of experimental investigations and comparisons with traditional methods.

CONTENTS

". . . . . fundamental standards should be readily accessible to all scientists amd engineers." A. H. Cook[1]

1. INTRODUCTION

Quantum metrology is an important branch of modern metrology (see, for example, Refs. 1 and 2). Its task is the development of new units of measurement of physical quantities and of the corresponding standards based on fundamental quantum relationships.

However, quantum methods have not as yet found wide application in photometry. This is something of a historical anomaly since, as a matter of fact, measurements of the spectral density of optical radiation began almost a century before the advent of quantum physics. One would expect that Einstein's quanta of light should long ago have become the natural units for measuring luminous energy. However, this did not happen, probably because suitable methods for the realization of the necessary standards have not been available.

The discovery of the parametric scattering of light[1)] in piezocrystals in 1967 (see, for example, Ref. 3) has resulted in the relatively unexpected and immediate availability of two convenient and relatively simple methods for the implementation of quantum photometry.[3,4]

The first method, i.e., measurement of the spectral radiance of the electromagnetic field, makes use of the following fundamental proposition in quantum electrodynamics: the ratio of the probabilities of stimulated and spontaneous emission in any particular field mode k is equal to the mean number of photons N_k in this mode. However, from the standpoint of photometry, N_k is none other than the spectral radiance I_k, expressed in certain dimensionless units. It follows that the ideal amplifier or converter of light that generates only quantum noise can be used to determine the spectral radiance of radiation incident upon it by measuring the signal-to-noise ratio. A piezocrystal pumped by coherent radiation is actually a device of this kind (parametric scattering may be looked upon as a manifestation of the quantum noise of a parametric frequency converter).

The basic feature of this technique is that it does not involve any particular standard (or reference), which makes this an *absolute* method, i.e., it does not rely on a standard. One way of looking at this is to say that the standard is provided by the omnipresent quantum fluctuations of the electromagnetic vacuum which, in a certain formal sense, give rise to spontaneous transitions. It is important to recall, however, that this approach is not consistent (see, for example, Refs. 5 and 6).

The second method—the calibration of photodetectors—also uses a relatively general relationship, namely, the connection between the statistics of a photocurrent and the radiation that generates it. The point is that certain types of radiation that can be referred to as calibrating radiation produce a photocurrent whose statistics contain information on the efficiency η of the detection process and on the average number N of photons entering the detector during the sampling time (see Ref. 7 for further details).

Here, too, parametric scattering has so far offered the optimum solution: it is a unique source of calibrating radiation that consists of a sufficiently intense and, importantly, highly directional flux of pair-correlated photons ("bipho-

 0038-5670/87/080716-08$01.80

tons"). This type of biphoton flux produces, with probability η^2, pairs of current pulses at the detector output. Their relative number is used to determine η and, hence, N. As in the first method, the measurement is performed in dimensionless units, and there is no need for calibrated standardizing devices. The method is therefore absolute.

The biphoton field produced by parametric scattering can also be used to calibrate electron-optic converters and vidicons. Moreover, it can be used to develop a standard source of frequency-tunable radiation that emits a given number of photons.[3,4]

It is important to note that, even before the discovery of parametric scattering, experiments were carried out on the calibration of detectors, using two-photon cascade radiation emitted by excited atoms (see Refs. 8 and 9 and the references cited therein). However, the precision of such measurements is low because of the absence of a rigid relationship between the photon momenta (due to the recoil of the atom). Methods relying on recording photon-electron coincidences suffer from the same defect.[10]

Two-photon cascade radiation has also been used to demonstrate the well-known Einstein, Podolsky, and Rosen paradox and to investigate hidden variable theories (see the reviews[11,12]). Here again, two-photon parametric radiation may be advantageous (see below, Fig. 5).

In the account given below, we present the main results of the first papers investigating promising methods of quantum photometry based on the parametric scattering effect.

2. NATURAL PHOTOMETRIC UNITS

The basic differential measure of noncoherent radiation—the spectral radiance I_k (or, more precisely, the spectral concentration of radiance) is defined in modern photometry as the energy transported per unit time, per unit spectral interval, per unit solid angle, per unit area. When the spectral interval is measured in units of wavelength, I_k has the dimensions of erg/cm^{3}sterad·s, whereas, when the spectral interval is measured in units of angular frequency, I_k has the dimensions of erg/cm^{2}sterad.

The thermal radiation of platinum at its melting point is used as the primary standard of I_k. The spectral radiance of thermal radiation is then calculated from Kirchhoff's law

$$I_k = \frac{\hbar c}{\lambda^3} A_k \left[\exp\left(\frac{\hbar\omega_k}{\varkappa T}\right) - 1\right]^{-1}; \qquad (1)$$

where A_k is the absorptive power and the index k labels the field modes. The latter includes the wave vector $\mathbf{k}$ and the type of polarization $\nu = 1, 2$ of the plane wave, i.e., $k = \{\mathbf{k},\nu\}$. The wave vector $\mathbf{k}$ also determines the direction $\mathbf{k}/|\mathbf{k}|$ and the natural mode frequency $\omega_k = c|\mathbf{k}| = 2\pi c/\lambda$. In general, I_k is also a function of position and of time (a rigorous electrodynamic definition of I_k is given in Ref. 13 and in the references cited therein).

Spectral radiance is used both for the characterization of the radiation itself and of the *sources* of this radiation. On the other hand, when *detectors* are calibrated, the total energy $\mathscr{E}$ incident on the detector in a time T is determined. The sensitivity of detectors is expressed in coulombs per joule, or the number of photoelectrons per joule, or some other analogous units.

When the units of physical quantities and the corresponding standardizing devices are chosen, it is obviously best to base this on the most fundamental concepts and phenomena. The *photon* and the *photon per mode* are such "natural" dimensionless units of energy and of the spectral radiance of optical radiation, respectively. The latter unit may be conveniently given a special name, for example, the *planck* (abbreviation—*pl*).

The relation between the average number N of photons and the number N_k of plancks (this number is also referred to as the *degeneracy factor* of the photon gas), and the more usual dimensional quantities, is

$$N = \frac{\mathscr{E}}{\hbar\bar{\omega}}, \quad N_k = \frac{I_k}{I_k^{\text{vac}}}, \qquad (2)$$

where $\bar{\omega}$ is the central frequency of quasimonochromatic radiation and $I_k^{\text{vac}} = \hbar c/\lambda^3$. The last quantity is the spectral radiance of radiation containing, on average, one photon in each mode. When the field is produced in vacuum, the field strength $\mathbf{E}(\mathbf{r},t)$ at each point in space-time fluctuates with the variance $\Delta E^2_{\text{vac}} = \langle \text{vac}|E^2|\text{vac}\rangle$, to which we can formally assign an energy of $\hbar\omega_k/2$ per mode, so that I_k^{vac} can be regarded as twice the spectral radiance of zero-point vacuum fluctuations: when $\lambda = 1$ μm, it is of the order of 0.6 W/Å cm^2 sterad.

Kirchhoff's law can now be written in the form

$$N_k = A_k N_k^{(0)}, \qquad (3)$$

where

$$N_k^{(0)} = \left[\exp\left(\frac{\hbar\omega_k}{\varkappa k}\right) - 1\right]^{-1} \qquad (4)$$

is the spectral radiance of thermal radiation emitted by a perfect black body and expressed in plancks. The last expression gives the relationship between the number of plancks and the effective (radiance) temperature of the radiation (Fig. 1).

We shall now describe the devices used to measure I and $\mathscr{E}$ directly in terms of the number of plancks and photons.

3. PARAMETRIC SCATTERING OF LIGHT

Parametric scattering can be readily observed by the unaided eye, e.g., when a lithium niobate crystal, about 1 cm thick, is illuminated by the blue light from an argon laser, producing an output power of the order of 1 W. The scattered radiation is mostly confined to the forward direction, close to the pump beam. In the far zone, it consists of concentric rings of green, yellow, and red light with an angular

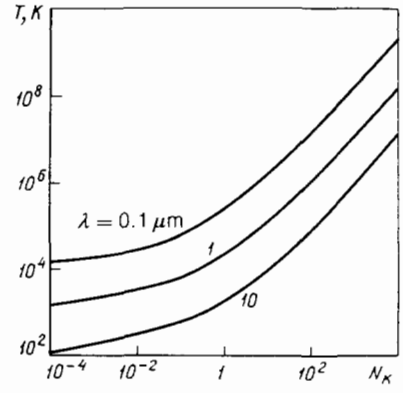

FIG. 1. Radiance temperature T of radiation as a function of the number of plancks, N_k, at different wavelengths λ.

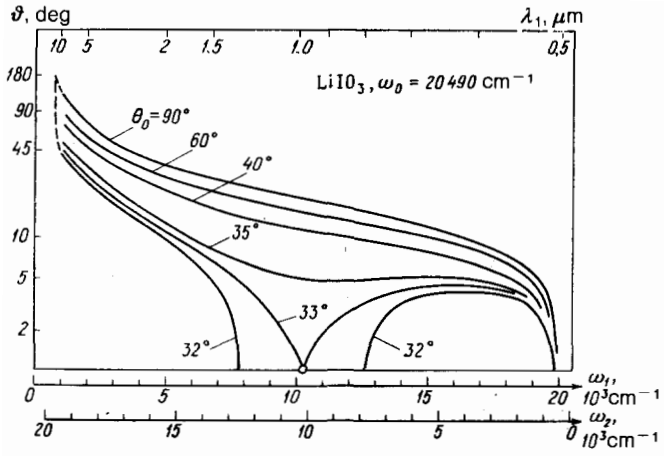

FIG. 2. Frequency and angular spectrum of parametric scattering in lithium iodate.

diameter from zero up to about 5°. The radiance temperature of this radiation exceeds 1000 K.

The effect is explained by the spontaneous decay of the monochromatic-pump photons into pairs of photons, $\omega_0 \to \omega_1 + \omega_2$, due to the macroscopic nonlinearity of the crystal. The significant point is that the scattering is not by the individual molecules,[2)] but by the entire excited region of the crystal as a whole. The result is that the photon momentum in the medium is strictly conserved: $\mathbf{k}_0 = \mathbf{k}_1 + \mathbf{k}_2$. This equation, referred to as the phase-matching condition, and the laws of frequency and angular dispersion $n^0(\omega)$ and $n^e(\omega,\theta)$ for the ordinary and extraordinary waves in the crystal, determine the observed angular dependence $\omega(\vartheta)$ of the frequency of the scattered radiation (Fig. 2).

When one of the two frequencies, for example, ω_2, lies in the region of strong infrared absorption by the crystal, the radiation intensity at this particular frequency is reduced. The intensity at the associated frequency $\omega_1 = \omega_0 - \omega_2$ is affected only to a small extent. Scattering in this part of the spectrum is referred to as *scattering by polaritons*. However, for photometry, we are interested only in the spectral region in which the crystal is transparent at all three frequencies. The phrase, "parametric scattering," will be understood to refer specifically to this case. The introduction of this special phrase is justified by the fact that the crystal emits diphotons, and not single photons as in other types of scattering. Moreover, parametric scattering is due to a purely electronic nonlinearity that exhibits no inertia.

From the point of view of photometry, it is very important to note that the directions and frequencies of the paired photons are related: when a photon is found in a particular mode $\mathbf{k}_1$, we may be sure that a photon will appear almost simultaneously in the associated mode $\mathbf{k}_2 = \mathbf{k}_0 - \mathbf{k}_1$. Of course, the time of appearance of a photon has an uncertainty Δt that does not exceed the reciprocal width of the spectrum. Similarly, transverse components of momentum are conserved during parametric scattering only to the diffractional accuracy of $|\Delta_{x,y}| < 1/a_{x,y}$, where $\boldsymbol{\Delta} = \mathbf{k}_0 - \mathbf{k}_1 - \mathbf{k}_2$ and $a_{x,y}$ are the transverse dimensions of the scattering region (usually determined by the cross section of the pump beam). The longitudinal components of momentum at small scattering angles $\vartheta_{1,2}$ are conserved to within $|\Delta_z| < 1/l$, where l is the length of the crystal in the direction of the pump beam. Hence, we obtain the phase-matching width (in frequency)

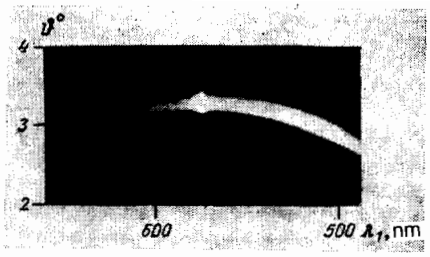

FIG. 3. Frequency and angular spectrum of spontaneous and stimulated parametric scattering (arc and bright point, respectively). The scattering angle is plotted along the vertical axis and the wavelength of the observed radiation along the horizontal axis. The stimulated signal at 17 540 cm^{-1} ($\lambda_1 = 0.57$ μm) is the result of beats between the argon laser ($\lambda_0 = 0.49$ μm) and the helium-neon laser ($\lambda_2 = 3.39$). The zero-point fluctuations of the infrared field play the part of the latter in the case of the spontaneous effect.

$$\frac{\Delta\omega}{2\pi} \simeq \frac{1}{l\,|u_1^{-1} - u_2^{-1}|} = \frac{1}{|\tau_1 - \tau_2|} \equiv \frac{1}{\Delta\tau}\ ; \qquad (5)$$

where u is the group velocity and τ the time taken by the photon to cross the crystal. The phase-matching width (5) determines the width of the parametric scattering spectrum [when the angular aperture of the recording equipment is small enough, so that $\vartheta_{det} \ll (d\vartheta/d\omega)\Delta\omega$]. The reciprocal of $\Delta\omega$ determines the order of magnitude of the possible delay of one photon relative to its associated photon, i.e., the second-order coherence time is $\Delta\tau = |\tau_1 - \tau_2|$. Thus, in lithium niobate with $l = 1$ cm, we have $\Delta\tau \sim 3$ ps and $\Delta\omega/2\pi c \sim 10$ cm^{-1}. In some cases, e.g., in the region of collinear phase matching (see the circle in Fig. 2), and also for $d\vartheta/d\omega = 0$ ($\lambda = 600$ nm at $\theta_0 = 33°$ in Figs. 2 and 3), the width $\Delta\omega$ is found to be greater by an order of magnitude or more.

When detectors are calibrated, it is important to ensure that the radiation consists of individual, nonoverlapping photon pairs. This condition is satisfied when the rate at which the recorded diphotons are produced is much smaller than $1/\Delta\tau$. When $\lambda_1 = \lambda_2 = 2\lambda_0$, this can be written in the form[3]

$$P_0 = \frac{c\lambda_0^4}{2\pi^5\delta\Omega\chi^2 l^2}\ ; \qquad (6)$$

where P_0 is the pump power, $\delta\Omega$ is the angular aperture of the recorded radiation, χ is the quadratic susceptibility of the crystal, and l is the length of the crystal.

When the entire parametric scattering spectrum is recorded, we have $\delta\Omega \sim 10^{-2}$ sterad.cm (Fig. 2). Let us suppose that $\lambda_0 = 0.5$ μm, $l = 1$ cm, and $\chi = 10^{-8}$ $(cm^3/erg)^{1/2}$, so that the field retains its two-photon structure for $P_0 \ll 30$ W. If, on the other hand, only one transverse mode is recorded, i.e., $\delta\Omega = 4\lambda_0^2/a_0^2$ (a_0^2 is the pump cross section), the formula given by (6) assumes the form $\Gamma^2 l^2 \ll 1$ or $P_0/a_0^2 \ll 30$ MW/cm^2. In these expressions, $\Gamma = \pi k_0 \chi E_0/2$ is the parametric amplification index and E_0 is the pump amplitude ($P_0 = ca_0^2 E_0/8\pi$). The condition that parametric amplification is small enables us to neglect stimulated processes ("parametric superradiance") that upset the diphoton character of the scattered field. The spectral radiance of the parametrically scattered field is then less than 1 *pl*, since precise phase matching ensures that $N_k = \Gamma^2 l^2$.

If, in addition to the pump, the crystal intercepts "idle" radiation with wave vector $\mathbf{k}_2$ satisfying the phase-matching condition, the latter will be amplified as it passes through the crystal at the expense of the pump energy (*parametric am-*

plification effect) and the crystal will emit "signal" photons in the mode $\mathbf{k}_1$ associated with $\mathbf{k}_2$ (*parametric frequency conversion* or *difference frequency generation*). This additional radiation, whose intensity is proportional to the spectral radiance I_k of the incident radiation, adds to the spontaneous emission that plays the part of the intrinsic quantum noise of the converter-amplifier. The colored rings mentioned above are then found to contain two bright "spots" in the directions of $\mathbf{k}_1$ and $\mathbf{k}_2$.

Figure 3 shows a photograph of the parametric scattering spectrum of a lithium iodate crystal, obtained by the crossed dispersion method. The intensity I_2 can be determined by comparing the intensity of the bright spot with that of the spontaneous background.

4. DETERMINATION OF THE EFFICIENCY OF PHOTODETECTORS

It is readily verified that the *a priori* information on the diphoton nature of the parametrically scattered field can be used in absolute measurements of the quantum yield of photodetectors, η, and, hence, to determine N and $\mathscr{E} = \hbar\bar{\omega}N$ in an arbitrary radiation field.[3,4,7]

Let us start with the single-channel method, in which the photon-counting photomultiplier intercepts part of the parametrically scattered radiation with approximately equal frequencies $\omega_1 \simeq \omega_2 \simeq \omega_0/2$ and opposite transverse momenta $k_{1x} \simeq -k_{2x}$ (Fig. 4). The photomultiplier then produces the usual "single-electron" pulse with probability $P_a = 2\eta(1-\eta)$ per diphoton. Much less frequently, i.e., with probability $P_b = \eta^2$, the photomultiplier produces "two-electron" pulses with amplitude greater by a factor of two as compared with the single-electron pulse (for simplicity, we are ignoring, for the moment, the fluctuations in the amplitude of output pulses, the noise pulses, and the possibility of two or more diphotons appearing during a single pulse). Suppose that M is the total number of diphotons reaching the photocathode during the measurement time T, so that, when T is large, the total number of ordinary pulses is $m_a = p_a M$ and the total number of double pulses is $m_b = P_b M$. Hence,

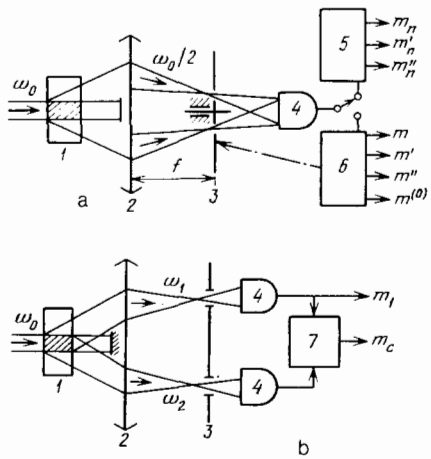

FIG. 4. Single-channel (a) and two-channel (b) methods of measuring photomultiplier efficiency: 1—piezocrystal, 2—objective, 3—mechanical modulator (diaphragm), 4—photomultiplier, 5—pulse-height analyzer, 6—four-channel synchronous detector, 7—coincidence circuit.

$$\eta = \left(1 + \frac{m_a}{2m_b}\right)^{-1}. \tag{7}$$

The significant point is that this formula is valid only when the photocathode does not receive single, unpaired photons. However, any optical element with linear transmission η_0 will partially break up the diphotons: single and paired photons will pass through it with probabilities P_a and P_b. For example, when $\eta_0 = 0.7$, 49 out of 100 diphotons will remain intact, 42 will be converted into single photons, and 9 will vanish altogether. This example shows that linear absorption not only reduces the average radiation energy but, in general, modifies its statistics, i.e., the form of the photon distribution function. This conclusion is also valid for the photoemission process: the photoelectron statistics can differ from the statistics of the original photons by more than mere scaling. This result was essentially used in (7) because, in the original diphoton field, the appearance of a pair of photons (one in each of the associated modes) has unit probability, and the probability of appearance of single photons is zero. It is clear from the foregoing that the parameter η defined by (7) includes not only the photomultiplier efficiency but also all the losses η_0 in the optical channel, including absorption and reflection in the piezocrystal itself. Effects associated with the fact that the crystal is not perfect are examined from the standpoint of quantum photometry in Refs. 14–17.

We note that two other possible methods of producing calibrating radiation, i.e., methods based on saturation and two-photon absorption effects, are considered in Ref. 7.

Another scheme that does not make use of the pulse-height amplitude analyzer is also possible. Here, one compares the total number of output pulses in two cases, namely, (1) the detector receives diphotons, in which case $m = m_a + m_b = \eta(2-\eta)M$ and (2) the objective has a mask in the focal plane (Fig. 4a), which transmits only one photon with $k_x > 0$ for each pair, in which case, $m' = \eta M$. The result is

$$\eta = 2 - \frac{m}{m'}. \tag{8}$$

In addition to the above two single-channel calibration scheme, there is also a two-channel scheme for measuring η, in which coincidences are counted (Fig. 4b). Here, the two photons in a pair are separated in frequency and/or direction, and each is recorded by its own photomultiplier. The appearance of a pulse in one of the photomultipliers (No. 1) while no pulse appears in the other (No. 2) signifies that the second photomultiplier has "transmitted" the photon. Consequently, the ratio of the number of coincidences m to the number of pulses m_1 in the first channel tends to the quantum yield of photomultiplier No. 2 when the time of measurement T is long: $m_c/m_1 = \eta_2$. Similarly, $m_c/m_2 = \eta_1$. The number of diphotons is determined by three counter readings: $m_1 m_2/m_c = M$. The relationship $m_c = \eta m_1$ was predicted in Ref. 18 and first confirmed in Ref. 19 (see also Refs. 21–23 and 29).

Frequency or angular filtration can be used [we recall that $\omega = \omega(\vartheta)$ in the case of parametric scattering] to determine the variance of the quantum yield $\eta(\omega)$ in a wide spectral range ($\omega < \omega_0$). When four-photon parametric scattering is used (two pump photons produce pairs of photons: $2\mathbf{k}_0 = \mathbf{k}_1 + \mathbf{k}_2$), the calibration range expands to $2\omega_0$.

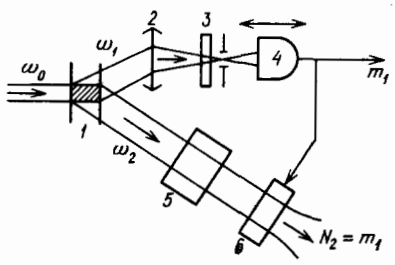

FIG. 5. Generator of a prescribed number of photons. The optical shutter 6 is opened only when pulses appear at the output of the photomultiplier 4; the number of photons, N_2, and the instants at which they are emitted can then be recorded. The delay line 5 can be a system of mirrors or a light guide. The frequency and space structure of the emitted photons can be varied by placing different masks and filters 3 in front of the photomultiplier, or by displacing the photomultiplier along the optical axis of the objective 2.

Parametric scattering can be used to calibrate analog photodetectors as well.[4,31] Moreover, a directional diphoton field due to parametric scattering can be used to develop a tunable standardizing source of radiation, producing a known number of emitted photons.[4] All that needs to be done in a two-channel device to determine η (Fig. 4b) is to replace photomultiplier No. 2 that is being calibrated with an optical shutter controlled by pulses from photomultiplier No. 1 (Fig. 5). One of the photons in the pair is then used to open the shutter transmitting the second photon, and to count the number of such events. We note that this device could provide a clear demonstration of the well-known Einstein, Podolsky, and Rosen paradox: by displacing the detector from the near zone[20] to the far zone, we can change the spatial structure of the radiated photon ($\Delta x \simeq 0 \to \Delta k_x \simeq 0$) without directly affecting it.

The diphotons produced in parametric scattering are created not only "simultaneously" (this manifests itself in the longitudinal pairing of the photons and the possibility of photomultiplier calibration), but also at a given "point" in the crystal, which should result in a transverse grouping and the possibility of absolute calibration of electron-optical converters, vidicons, and even (in principle) photographic materials.[20] Transverse grouping can be detected by focusing the image of the crystal in scattered light on the photocathode of an electron-optical converter. The image on the converter screen then partially consists of paired or closely spaced luminous points, with minimum average separation given by the uncertainty relation $k_x \Delta x \gtrsim 1$ or $\Delta x \gtrsim \lambda / \vartheta_{\max}$, where $2\vartheta_{\max}$ is the angular width of the recorded radiation. The efficiency of the converter can be determined by counting the number of such pairs of points (subject to the condition that the converter is capable of exhibiting the photon structure of the image).

The experimental implementation of the above three schemes (see Fig. 4) is described in Refs. 16, 21, and 22. The quantum efficiency η was measured for a large number of photomultipliers of different types. Some had amplitude characteristics with a well-defined single-electron maximum, whereas others were found to have exponential characteristics with enhanced dark current. Table I lists some of the experimental results for $\lambda = 650$ nm together with the certified integrated sensitivity S and the η_{cert} calculated from it for $\lambda = 650$ nm (the conversion was based on a typical spectral sensitivity curve of a multialkali cathode).

TABLE I. Absolute measurement of the photomultiplier efficiency.[16,21]

Photodetector	S, mA/lm	quantum efficiency, %		
		Nominal	One channel	Two channels
FEU-79	0.31	7.8	3.6	3.8
Ditto	0.23	6.0	3.3	3.0
"	0.20	5.3	1.8	—
Quantocon C31034 A (USA)	0.7	18	7.0	7.5

The striking result is that the two single-channel schemes agree to within experimental uncertainty. The spread of the measurements is of the order of $\Delta\eta \sim 10^{-3}$ for a measurement time of 1 h, which corresponds to the Poisson variance. These results have been corrected for the transmission coefficient η_0 of the optical channel, which is determined in independent relative measurements.

We note that the certified efficiency is systematically higher than the measured efficiency, while the difference between the experimental data obtained by the three methods is slight. This systematic difference may be due to some ageing effects (the age of these devices was about 10 years).

In addition, the two-channel method was used to determine the variance $\eta(\omega)$ (Fig. 6). We note that the diphoton field generator that incorporates the single-crystal lithium niobate pumped by the helium-cadmium laser (325 nm) can be used, at least in principle, to carry out measurements in the range 0.35–4 μm (determined largely by the transparency range of the crystal).

Let us now consider some of the features of the experiment. The formula given by (7) cannot be used directly because of fluctuations in the amplitude of the photomultiplier output pulses. The NTA 1024 multichannel pulse-height analyzer was therefore used to record the number m_n of pulses with different amplitudes (n is the channel number). The counts were recorded sequentially at equal time intervals T for four positions of the diaphragm that filters the diphoton radiation according to the transverse momentum k_x (Fig. 4a). Four sets of numbers were obtained as a result, namely, $m_n^{(0)}$, m_n, m_n', m_n''. This corresponded to the follow-

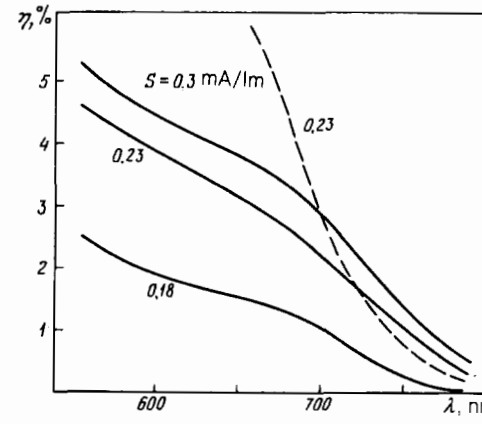

FIG. 6. Variance of quantum efficiency of different examples of the FEU-79 photomultiplier, measured by the two-channel method.[16,22] The numbers shown against the curves are the nominal (certified) integrated sensitivities S in mA/lm. The broken curve represents calculations for a multialkali photocathode with $S = 0.2$ mA/lm.

ing situations: (1) radiation completely cut off, (2) diphotons incident on the cathode, (3) one photon with $k_x > 0$ selected from each diphoton, and (4) same as (3) but with $k_x < 0$.

Let g_n be the normalized distribution of single-electron pulses from a given photomultiplier, as observed under weak illumination after subtraction of dark counts. Let us suppose that, when two photoelectrons are emitted simultaneously from the cathode, the distribution is $0.5g_{n/2}$. Instead of (7) and (8), we then have

$$\eta = \frac{\tilde{m}'_{2n} + \tilde{m}''_{2n} - \tilde{m}_{2n}}{2\tilde{m}'_{2n} - (\tilde{m}'_n/2)}; \quad (9)$$

where the tilda indicates that the dark count $m_n^{(0)}$ has been subtracted and, by definition, $m''_n > m'_n$ (because the diaphragm is asymmetric). Table I lists the values obtained by this procedure by averaging (9) over about 200 channels with n lying in the region of the single-electron maximum.

We note that these were actually the first experiments to record the two-electron photoeffect due to photon pairing.

In the other variant (one detector without analyzer), we made use of a four-channel digital synchronous detector incorporating a mechanical modulator (disk with slots of a particular shape, with rotation axis lying along the optical axis of the system), a reference voltage generator with a period of about 1 s, four counters, and a switching circuit for them. The counters recorded the total number of pulses under the above conditions. Suppose that $m'' > m'$. Instead of (8), we then have

$$\eta = \frac{1}{\tilde{m}'} (\tilde{m}' + \tilde{m}'' - \tilde{m}). \quad (10)$$

Typical counting rates were as follows: $\dot{m}(0) \sim 100\ \text{s}^{-1}$, $\dot{m}' \sim \dot{m}'' \sim \dot{m}/2 \sim 3 \times 10^3\ \text{s}^{-1}$. The Poisson uncertainty for $T = 1$ h was $\Delta\eta = 4(m')^{-1/2} \sim 10^{-3}$.

The two-channel system (see Fig. 4b) included two identical pulse-shaping and amplification channels, and a coincidence circuit with a resolution of $\Delta t \sim 4$ ns. Random coincidences could be ignored because their relative contribution was equal to the ratio of Δt to the average interval of time between photons incident on the photomultiplier: $\eta_1/\dot{m}_1 \sim 10^{-5}$ s [see (9)]. When $\eta_2 = m_c/m_1$ was determined, it was important to ensure that the frequency and angular bands of channel 2 easily covered all the modes associated with modes in the reference channel 1. Control measurements showed that the ratio m_c/m_1 was independent of pump intensity, optical losses, and reduction in channel width of channel 1.

5. MEASUREMENT OF SPECTRAL RADIANCE

As already noted, measurements of radiance by the parametric scattering method are based on the comparison between signals due to spontaneous and stimulated scattering. For a perfect crystal, $m_1 = C$ and $m'_1 = C(N_2 + 1)$, where C is the proportionality factor that depends on pump intensity, nonlinearity of the crystal, detector efficiency, and so on. Hence, the spectral radiance of low-temperature radiation incident on the crystal, expressed in plancks, is determined by the signal-to-noise ratio in the signal channel:

$$N_2 = \left(\frac{m'_1}{m_1} - 1\right) \varkappa; \quad (11)$$

where $\varkappa$ is a correction coefficient taking into account the Fresnel reflection by crystal faces ($R_i \neq 0$) and its nonideal transparency ($\alpha_i \neq 0$), which is particularly significant for the idler wave, which usually lies in the infrared. This coefficient is calculated in Ref. 14 in the plane-wave approximation, using a phenomenological relationship between spontaneous and stimulated scattering that generalizes (3) but is proved only for $\alpha_0 = \alpha_1 = 0$ (Ref. 3). A more general expression for $\varkappa(R_i, \alpha_i, n)$ that takes into account absorption at all three frequencies and an arbitrary number of reflections, n, was obtained by Kitaeva[17,24] from the following heuristic rule: spontaneous parametric scattering in an absorbing medium is satisfactorily described by the classical theory if one adds one fictitious photon to each incident idler mode.

The values of $\varkappa$ for different waves are given in Ref. 24 for a number of crystals. The frequency and angular characteristics of these crystals are also reported in Ref. 24. It is found that gadolinium molybdenate has the lowest $\varkappa$: $\varkappa = 1.1$ for $l = 1$ cm and $\lambda_2 = 2$–$5\ \mu$m.

It is important to note that the "parametric photometer" will yield reasonably accurate values of radiance for a reasonable time of measurement, but only above a certain minimum value of N (of the order of $0.01\ pl$). The minimum effective radiance temperature rises, accordingly, from 100 to 10^4 K as the wavelength is reduced from 10 μm to 0.1 μm (Fig. 1).

The first experimental verification of (11) is described in Ref. 25. Table II summarizes the main results of this verification. Independent estimates of the spectral radiance, performed by traditional methods, were found to agree with these results to within experimental uncertainty. The principle of the experimental arrangement is illustrated in Fig. 7. Two types of experiment were performed, namely, with low-temperature continuous radiation of low radiance ($\lambda_2 \sim 4$ μm) and with high-temperature pulsed radiation ($\lambda_2 \sim 0.5$ μm).

The source of continuous radiation was the hot-filament lamp KGM-12-100 with a tungsten wire and iodine cycle, and an argon laser was used for pumping. The idler wavelength lay in the 4-μm range to ensure that the stimulated effect amounted to something of the order of 1% against the spontaneous-scattering background (Fig. 1). Radiation

TABLE II. Absolute measurement of radiance.[25]

Crystal	λ_0, μm	λ_1, μm	λ_2, μm	Measured radiance		
				In plancks	In W/Å·cm²sterad	In kelvins
Lithium niobate	0.46	0.51	3.9	0.024±0.006	$1.6 \cdot 10^{-5}$	980±70
KDP	0.27	0.53	0.53	18±4	250±50	$5 \cdot 10^5$
KDP	0.27	0.51	0.56	—	2.2±0.5	$7 \cdot 10^4$

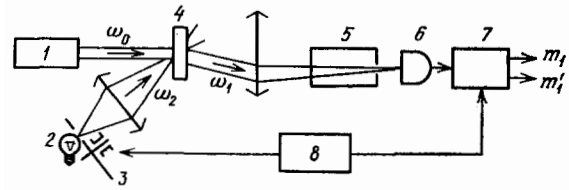

FIG. 7. Parametric photometer: 1—pump laser, 2—source being calibrated, 3—modulator, 4—nonlinear crystal, 5—monochromator, 6—photodetector, 7—synchronous detector, 8—control unit.

from the lamp was projected onto a crystal in such a way that all the modes coupled to the signal modes by the phase-matching condition, and recorded by the receiving system, were easily filled. The receiving system incorporated an FEU-79 photomultiplier and a photon counter. The idler and signal waves propagated inside the crystal at angles $\vartheta_2 = 28°$ and $\vartheta_1 = 3°$ to the pump beam. The latter was perpendicular to the optical axis of the crystal and to its working faces. The spectral resolution was $\Delta\lambda_2 = 12$ nm and the angular resolution $\Delta\vartheta_2 = 3°$. Independent measurements of the luminance of the lamp were carried out with a pyrometer whose readings were converted to the infrared region with allowance for the dispersion of the tungsten grayness factor. This procedure introduced a considerable uncertainty, exceeding 30%.

In the pulsed method, the pump was the fourth harmonic of the Q-switched neodymium laser. The pulse length was 5 ns and the power a few tens of kilowatts. The signal radiation was recorded by a FEU-39 photomultiplier and an analog-to-digital converter.

The radiance of two pulsed sources of radiation was determined, i.e., the second harmonic of the pump laser and the luminescence of a rhodamine-6G dye pumped by the same harmonic.

When the radiance of the harmonic was measured, the spectral band of the measured radiation (0.15 Å) was less than the converter bandwidth (40 Å), i.e., all the modes coupled to the recorded modes were not uniformly filled. The radiance values listed in Ref. 25 (see Table II for the case $\lambda_1 = \lambda_2 = 0.53$ μm) were therefore too low by the factor $40/0.15 = 233$. The interaction was almost collinear: $\vartheta_1 = \vartheta_2 = 3.3°$.

Independent estimates of the emitted luminescence

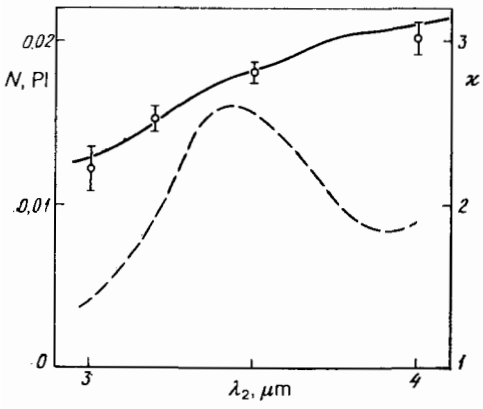

FIG. 8. Comparison between the two methods of measuring the spectral radiance N of the hot-filament lamp in the infrared range.[26] Points—absolute method, solid line—pyrometric method (corrected for dispersion of the absorptive power of tungsten), broken line—variance of the correction factor $\varkappa$ in (11).

were based on the output power (3 kW), quantum yield (0.83), luminescence band width (30 nm), and effective area of source (0.13 cm^2).

The experiment with the hot-filament lamp was subsequently repeated with a number of improvements.[26,32] An argon laser (488 nm, 0.1 W), a KGM-24-150 lamp, a lithium iodate crystal, and a DMR-4 monochromator with a bandwidth of $\Delta\lambda_1 = 2$–4 nm were employed. The signal-to-noise ratio was measured at several points in the range 3–4 μm. In the same range, a determination was made of the correction factor $\varkappa(\lambda_2)$ and of the spectral radiance of the lamp $N(\lambda_2)$, using corrected pyrometer readings in which the estimated uncertainty was 10%.

Figure 8 compares the values of N_2 obtained by the two methods. Good agreement between values found by the two fundamentally different methods in a wide spectral interval (in which $\varkappa$ varies by a substantial factor) confirms the validity of (11).

6. CONCLUSION

The first results obtained by the two possible methods of quantum photometry, summarized above, suggest that they could be used as a basis for laboratory instruments used in absolute measurements of intensity and photodetector calibrations. It may well be that the diphoton field produced in parametric scattering will eventually be used in studies of the psychophysiology of vision and of multiphoton and ultrafast processes.

It is important to note, however, that the above methods suffer from a number of disadvantages. The fundamental point is that it is essential to introduce the correction $\varkappa(\alpha,R)$ [see (11)] for the fact that the converter crystal is not ideal (although the uncertainty introduced thereby can apparently be made less than 1%). It is also necessary to take into account possible instability of $\varkappa$ in time, due to heating and ageing of the crystal. The low coefficient of conversion ($< 10^{-7}$) of the pump radiation into useful spontaneous radiation requires high-grade optical elements and careful adjustment. Absolute measurement of radiance in the visible range is restricted to high-temperature radiation ($T > 10^4$ K).

Further studies will, of course, be necessary to elucidate the usefulness of primary standards based on parametric scattering. The undoubted advantages of parametric radiance standards include their absolute character and the absence of uncertainties due to temperature measurement and grayness coefficient in the wide spectral range 0.3–12 μm, depending on the type of crystal and pump wavelength (if currently existing crystals and lasers are employed).

It would be interesting to investigate other nonlinear optics phenomena suitable for quantum photometry, for example, hyperparametric scattering[3] and the saturation effect.[7]

According to Kirchhoff's formula (1), it is possible to produce an absolute pyrometer for temperature measurements. It would be interesting to compare one of the reference points on the accepted temperature scale (for example, the melting point of gold) with the readings of the absolute pyrometer.

We note that the phenomena examined here admit of a phenomenological description[3,4,27] that generalizes Kirchhoff's law (which is valid only within the framework of lin-

ear and geometric optics). On the other hand, these phenomena are described by very general relationships of quantum electrodynamics, and their careful study may be of independent interest. For example, Shepelev[28] has shown that absolute measurement of the spectral radiance of synchrotron radiation, which can also be calculated quite accurately, can be used to determine the fine structure constant in terms of relative measurements alone.

[1)]Also known as parametric luminescence, optical parametric noise, frequency splitting effect, spontaneous parametric frequency down-conversion, and so on.

[2)]Scattering by individual molecules also occurs, but the scattered intensity is much lower and is virtually isotropic (see Ref. 30, for example).

[1]A. H. Cook, Rep. Prog. Phys. **35**, 463 (1972).
[2]P. H. Cutler and A. A. Lucas (Eds.), Quantum Metrology and Fundamental Constants, Plenum, 1981 [Russ. transl., Mir, M., 1981].
[3]D. N. Klyshko, Photon and Nonlinear Optics [in Russian], Nauka, M., 1980.
[4]D. N. Klyshko, Kvantovaya Elektron. (Moscow) **4**, 1056 (1977) [Sov. J. Quantum Electron. **7**, 591 (1977)].
[5]V. L. Ginzburg, Usp. Fiz. Nauk **140**, 687 (1983) [Sov. Phys. Usp. **26**, 713 (1983)].
[6]R. P. Puri, J. Opt. Soc. Am. B **2**, 447 (1985).
[7]D. N. Klyshko, Zh. Eksp. Teor. Fiz. **90**, 1172 (1986) [Sov. Phys. JETP **63**, 682 (1986)].
[8]A. N. Zaĭdel' and E. Ya. Shreĭder, Vacuum Spectroscopy [in Russian], Nauka, M., 1976.
[9]E. S. Fry, Phys. Rev. A **8**, 1219 (1973).
[10]R. McAdams and S. K. Srivastava, Appl. Opt. **22**, 1551 (1983).
[11]B. I. Spasskiĭ and A. V. Moskovskiĭ, Usp. Fiz. Nauk **142**, 599 (1984) [Sov. Phys. Usp. **27**, 273 (1984)].
[12]A. A. Grib, *ibid.* **142**, 619 (1984) [Sov. Phys. Usp. **27**, 284 (1984)].
[13]L. A. Apresyan and Yu. A. Kravtsov, Usp. Fiz. Nauk **142**, 689 (1984) [Sov. Phys. Usp. **27**, 301 (1984)].
[14]G. Kh. Kitaeva, D. N. Klyshko, and I. V. Taubin, Kvantovaya Elektron. (Moscow) **9**, 561 (1982) [Sov. J. Quantum Electron. **12**, 333 (1982)].
[15]A. A. Malygin and A. V. Sergienko, Preprint No. 5294-84 [in Russian], VINITI AN SSSR M., 1984.
[16]A. A. Malygin, Photon Bunching in Parametric Light Scattering and Its Metrological Applications. Author's Thesis for Candidate Phys.-Mat. Sci. [in Russian], Moscow State University, 1984.
[17]G. Kh. Kitaeva, Parametric Frequency Conversion as a Method of Absolute Determination of Spectral Radiance. Author's Thesis for Candidate Phys.-Mat. Sci. [in Russian], Moscow State University, 1982.
[18]B. Ya. Zel'dovich and D. N. Klyshko, Pis'ma Zh. Eksp. Teor. Phys. **9**, 69 (1969) [JETP Lett. **9**, 40 (1969)].
[19]D. C. Burnham and D. L. Weinberg, Phys. Rev. Lett. **25**, 84 (1970).
[20]D. N. Klyshko, Zh. Eksp. Teor. Phys. **83**, 1313 (1982) [Sov. Phys. JETP **56**, 753 (1982)].
[21]A. A. Malygin, A. N. Penin, and M. V. Sergienko, Pis'ma Zh. Eksp. Teor. Phys. **33**, 493 (1981) [JETP Lett. **33**, 477 (1981)].
[22]A. A. Malygin, A. N. Penin, and A. V. Sergienko, Kvantovaya Elektron. (Moscow) **8**, 1563 (1981) [Sov. J. Quantum Electron. **11**, 839 (1981)].
[23]A. A. Malygin, A. N. Penin, and A. V. Sergienko, Dokl. Akad. Nauk SSSR **281**, 308 (1985) [Sov. Phys. Dokl. **30**, 227 (1985)].
[24]O. N. Abroskina, G. Kh. Kitaeva, and A. N. Penin, Kvantovaya Elektron. (Moscow) **12**, 877 (1985) [Sov. J. Quantum Electron. **15**, 577 (1985)].
[25]G. Kh. Kitaeva, A. N. Penin, V. V. Fadeev, and Yu. A. Yanait, Dokl. Akad. Nauk SSSR **247**, 586 (1979) [Sov. Phys. Dokl. **24**, 564 (1979)].
[26]O. N. Abroskina, G. Kh. Kitaeva, and A. N. Penin, *ibid.* **280**, 584 (1985) [Sov. Phys. Dokl. **30**, 67 (1985)].
[27]D. N. Klyshko, *ibid.* **244**, 563 (1979) [Sov. Phys. Dokl. **24**, 39 (1979)]; Izv. Akad. Nauk SSSR Ser. Fiz. **46**, 1478 (1982) [Bull. Acad. Sci. USSR Phys. Ser. **46** (8), 33 (1982)].
[28]A. V. Shepelev, Vestn. Mosk. Univ. III. Fiz. Astron. **25**, 3 (1984).
[29]C. H. Hong and L. Mandel, Phys. Rev. Lett. **56**, 58 (1986).
[30]N. B. Baranova and B. Ya. Zel'dovich, Zh. Eksp. Teor. Fiz. **71**, 727 (1976) [Sov. Phys. JETP **44**, 383 (1976)].
[31]A. N. Penin and A. V. Sergienko, Pis'ma Zh. Tekh. Fiz. **12**, 795 (1986) [Sov. Tech. Phys. Lett. **12**, 328 (1986)].
[32]O. N. Abroskina, G. Kh. Kitaeva, and A. N. Penin, Izm. Tekh. **3**, 14 (1986).

Translated by S. Chomet